Mathematical Modelling and Control

http://www.aimspress.com/journal/mmc

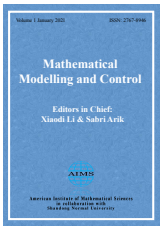

MMC, 3(4): 416–434.
DOI: 10.3934/mmc.2023033
Received: 24 June 2023
Revised: 10 October 2023
Accepted: 22 November 2023
Published: 28 December 2023

Research article

Modeling the vaccination control of bacterial meningitis transmission dynamics: a case study

Monica Veronica Crankson[1], Olusegun Olotu[2], Ayodeji Sunday Afolabi[2] and Afeez Abidemi[2,*]

[1] Department of Mathematical Sciences, University of Mines and Technology, Box 237, Tarkwa, Ghana

[2] Department of Mathematical Sciences, Federal University of Technology, Akure, P. M. B. 704, Akure, Ondo State, Nigeria

* **Correspondence:** Email: mcrankson@umat.edu.gh; Tel: +233504883208.

Abstract: Bacterial meningitis, which is considered a major concern by the World Health Organization, is a medical emergency that lingers as a terrifying infection in sub-Saharan Africa and other countries in the "meningitis belt" due to the frequent occurrence of the infection and its debilitating effects among survivors, even after treatment. This study presents a novel two-strain compartmental bacterial meningitis model. The disease-free equilibrium was established to be locally and globally asymtotically stable. Numerical simulations were performed to visualize the effects of various model parameters on each compartment. Sensitivity analysis was also performed and it was established that the most sensitive parameter for both strains 1 and 2 is the transmission probability, β. It was ascertained that bacterial meningitis will not spread in the population if at least 25% of the population are immune to the disease.

Keywords: novel two-strain bacterial meningitis; streptococcus pneumoniae; neisseria meningitidis; vaccination

1. Introduction

Meningitis is a disease of the central nervous system that leads to soreness of the lining around the brain and spinal cord. It is an acute inflammation of the defensive membranes covering the brain and spinal cord, collectively known as the meninges. This occurs when fluid surrounding the meninges is infected. Meningitis may be fatal because of the severe nature of inflammation of the brain and spinal cord, so the illness is treated as a medical emergency [1]. If not treated immediately, it can lead to permanent disability, coma, brain swelling, or even death. It is mainly detected by a lumbar puncture where a needle is used to extract a sample of cerebrospinal fluid from the spinal canal. It can also be diagnosed by brain imaging such as computerized tomography scan or magnetic resonance imaging, swab of fluid from the nose or throat, and blood and urine testing [2].

Meningitis infections can be caused by different pathogens, but most of these infections are attributed to virus, which is the least serious type with the next common cause being bacteria, fungi and parasites [3]. Bacterial meningitis is the most severe and epidemic-prone disease, affecting a significant part of the world's population. The bacteria are present worldwide, although in Africa, the disease is endemic to the meningitis belt. The meningitis belt spans from the Atlantic Ocean to the Red Sea, semi-arid area of sub-Saharan Africa. There is also a high tendency for outbreaks to spread across countries due to the insecure state of African borders. Other sub-Saharan African countries have also recorded large outbreaks [4].

Case fatality rates, which are often between 1 and 2 days after the onset of symptoms, may be as high as 50–80% when not treated and approximately 8–15% when treated [5]. The northern part of Ghana, namely, the Northern, North East, Savannah, Upper East and Upper West regions, lies completely in the meningitis belt and has

experienced recurrent outbreaks, often during dry weather seasons characterized by low humidity, high temperatures and abundance of dust. The Brong Ahafo, Bono East and upper parts of the Volta region have also recorded sporadic cases [6].

Figure 1 shows the geographic distribution of meningitis in West African affected countries.

Figure 1. Areas of Africa with frequent epidemics of meningitis [7].

Bacterial meningitis was initially transmitted from an animal to a human being but has since become a person-to-person transmission through infected air droplets, saliva, respiratory secretions and direct contact with contaminated surfaces. The infection spreads easily when an infected person comes into close proximity or has long-term contact with others. Staying in overcrowded housing, attending sports or cultural events, sharing utensils, coughing, sneezing and kissing can all contribute to disease outbreaks [8].

Bacterial meningitis is caused by some strains of bacteria such as Streptococcus pneumoniae (pneumococcus), Neisseria meningitidis (meningococcus), Haemophilus influenzae (Haemophilus) and Listeria monocytogenes (Listeria). Neisseria meningitidis, Streptococcus pneumoniae and Haemophilus influenzae type B were the most common bacteria, accounting for over 80% of all bacterial meningitis cases. Meningitis caused by Haemophilus influenzae type B is much less common, now that the Haemophilus influenzae type B vaccine is administered to all children as part of routine immunization [1].

Most patients recover well after prompt treatment; however, several patients experience severe health complications even after prompt treatment. These complications include hearing impairments, neurological disabilities and loss of limb function [9]. The estimated risk of at least one complication after recovery is nearly 4 out of every 10 patients, with a median risk of approximately 20% in such patients [10].

The awareness of bacterial meningitis as a vaccine-preventable disease is commendable, but a number of people may not know that these vaccines are strain specific. Several previous researchers have used mathematical models to analyze the transmission and control dynamics of bacterial meningitis [11–14]. For models that consider vaccination, there is a common assumption that the vaccine does not confer immunity to all recipients, and is used as a means of treatment for infected people. However, this assumption must be lifted, as it is nowhere close to the real-life situation where the available vaccines confer varying degrees of duration of immunity against the specified strain. Furthermore, these specific vaccines are used for prevention (routine immunization) and in response to outbreaks (prompt reactive vaccination) but not for treatment [15].

The dynamics of cerebrospinal meningitis in the Jirapa district of the Upper West region of Ghana was presented via mathematical modeling by [13]. The existence of a solution to the model and its stability were examined. It was discovered that early treatment, adherance to cerebrospinal meningitis protocols, and the combined efforts of medical personnel and traditional healers could help control the disease.

In [16, 17], an age-structured mathematical model of meningitis A (MenA) transmission, colonization and disease in the African meningitis belt was formulated and used to investigate the effects of various vaccination strategies. The validity of the model was assessed by comparing the simulated incidence of invasive MenA and the prevalence of MenA carriage with the observed incidence and carriage data. The model was able to reproduce the observed dynamics of MenA epidemics in the African meningitis belt, including seasonal increases in incidence, with large epidemics occurring every 8–12 years. It was established that the most effective modeled vaccination strategy is to

conduct mass vaccination campaigns every 5 years for children aged 1–5 years.

Research [18] also used mathematical models to identify the crucial factors determining the dynamics of meningitis. Their simulated results suggest that temporal population immunity plays a key role and should be considered during disease monitoring and assessment of the efficiency of the vaccines deployed. A deterministic model for meningococcal meningitis transmission dynamics with variable total population size was presented in [19]. It was shown analytically and numerically that the disease can be eradicated using effective control measures. Their simulation suggested control measures that can reduce the disease transmission rate and immunity waning rate, as well as boost the vaccination and treatment rates.

A discrete mathematical model for the spread of meningococcal meningitis using cellular automata on graphs was presented in [20]. The discrete nature of the mathematical objects used in the algorithm renders model implementation simple and efficient. It was concluded that both the individual and global behaviours of the disease could be determined.

Research [21] presented a nonlinear deterministic model on the dynamics of bacterial meningitis by incorporating time-dependent controls. Their results showed that carriers had a more significant effect on disease transmission than did the infectious class. This can be attributed to the fact that symptomatic patients are often admitted during the acute phase of the infection. This model was formulated as an optimal control problem to determine the optimal strategies for disease control. It was ascertained that vaccination played a key role in curtailing the spread of the disease. Hence, stakeholders are admonished for pushing for existing or new vaccines and antibiotics to be disbursed in the most affected areas.

To study the dynamics of the 2017 meningitis outbreak in Nigeria, [22] presented a deterministic model for meningitis caused by Neisseria meningitidis. This model was used to investigate the optimal strategy for curtailing the disease spread. The results indicated that combining the two control variables is the most cost-effective strategy because it averts more infections at low costs.

Because the after-effects of meningitis are not always pleasant, [23] presented a susceptible-vaccinated-carrier-infected-recovered-susceptible model to study the dynamics of meningitis. They distinguished between those who recovered with disabilities and those who did not. Their model suggests that a high vaccine uptake rate could control the disease. As an extension of the model for incorporating the treated population, an susceptible-vaccinated-carrier-infected-recovered deterministic compartmental model of the transmission dynamics of bacterial meningitis was presented in [24]. The numerical simulation results demonstrated the effects of the model parameters on each compartment, and established that efficient and effective vaccination and treatment are crucial for disease control.

Even with the availability of drugs and vaccines in the management of meningitis outbreaks, case fatality rate in Ghana remain high ranging between 36–50% [25]. In this study, a novel two-strain deterministic model based on the susceptible-vaccinated-carrier-infected-recovered is developed with new model parameters to obtain a more realistic model.

2. Model formulation

To formulate the model, a wide range of parameters was used to incorporate the coexistence of two bacterial meningitis strains: Streptococcus pneumoniae and Neisseria meningitidis. It is evident that the available vaccines are strain-specific [26], making the risk of contracting an infection from a strain one has not been vaccinated against great concern. In the proposed model, the total population at time t, denoted by $N(t)$, is divided into nine mutually exclusive epidemiological classes: the susceptible class $S(t)$ that can contract strains 1 and 2, vaccinated classes $V_1(t), V_2(t)$, carrier classes $C_1(t), C_2(t)$, infected classes $I_1(t), I_2(t)$, and two recovered classes $R_1(t)$ and $R_2(t)$. Thus, $N(t)$ is given by

$$\begin{aligned} N(t) =& S(t) + V_1(t) + V_2(t) + C_1(t) + C_2(t) \\ &+ I_1(t) + I_2(t) + R_1(t) + R_2(t). \end{aligned} \tag{2.1}$$

The susceptible class is a population that has not yet been infected and has not received any vaccine against the disease. This is generated by the birth or recruitment rate α and the loss of immunity acquired through previous

vaccinations at waning rates ω_1, ω_2. The susceptible population is reduced by infection through effective contact with infected individuals at rates λ_1 and λ_2, which are defined as

$$\lambda_1 = \frac{\beta[\eta C_1(t) + I_1(t)]}{N(t)}, \tag{2.2}$$

$$\lambda_2 = \frac{\beta[\eta C_2(t) + I_2(t)]}{N(t)}, \tag{2.3}$$

where β is the effective transmission probability per contact and $0 < \eta \leq 1$ is a modification parameter indicating the infectiousness of individuals in the carrier class. The population is also reduced by the natural death rate μ and the vaccination rates θ_1, θ_2. Hence, the rate of change of the susceptible population is represented by the ordinary differential equation (ODE):

$$\frac{dS}{dt} = \alpha + \omega_1 V_1 + \omega_2 V_2 - (\lambda_1 + \lambda_2 + \theta_1 + \theta_2 + \mu)S. \tag{2.4}$$

The vaccinated class was divided into two based on the vaccines available against the two strains considered. The vaccinated population with immunity to strain 1 received pneumococcal conjugate vaccines as a form of protection against disease. This population is increased by the vaccination of susceptible individuals at rate θ_1. On average, pneumococcal conjugate vaccines take 2 weeks to fully kick in and should protect up to 5 years. As this vaccine does not confer immunity to all strains of bacteria causing meningitis, vaccinated individuals of strain 1 may be infected by another strain, but at a lower rate than unvaccinated individuals. This population is decreased by exposure to the disease or by vaccine waning and natural death. Therefore, the rate of change in the vaccinated population with immunity to strain 1 is represented as

$$\frac{dV_1}{dt} = \theta_1 S - (1 - \epsilon_1)\lambda_1 V_1 - (\lambda_2 + \omega_1 + \mu)V_1, \tag{2.5}$$

where $0 \leq \epsilon_1 \leq 1$ is the level of efficacy of the pneumococcal conjugate vaccine.

The vaccinated population with immunity to strain 2 is the population of individuals who received meningococcal conjugate vaccines as a form of protection from the disease. This population is increased by vaccination of susceptible individuals to this specific strain at a rate of θ_2. Individuals often develop immunity within 2 weeks of receiving meningococcal conjugate vaccines and should protect them for 3–5 years. Because this vaccine does not confer immunity to all strains of bacteria causing meningitis, vaccinated individuals of strain 2 may be infected with strain 1 at an effective contact rate λ_1, but at a lower rate than unvaccinated individuals. This population is decreased by exposure to infection $(1-\epsilon_1)\lambda_1$ or by vaccine waning ω_2 and natural death μ. Thus, the rate of change of the vaccinated population with immunity to strain 2 is given as

$$\frac{dV_2}{dt} = \theta_2 S - (1 - \epsilon_2)\lambda_2 V_2 - (\lambda_1 + \omega_2 + \mu)V_2, \tag{2.6}$$

where $0 \leq \epsilon_2 \leq 1$ is the level of efficacy of the meningococcal conjugate vaccine.

The carrier population of strain 1 is made up of a population infected with Streptococcus pneumoniae but does not show any signs or symptoms even though they are infectious. This is generated by the effective contact rate λ_1 and decreased as a result of the population becoming symptomatic at rate σ_1. This population is decreased by the recovery rate γ_{C1} and natural death rate μ. Consequently, the rate of change in the carrier population of strain 1 is expressed as

$$\frac{dC_1}{dt} = \lambda_1(1-\tau_1)S + (1-\epsilon_1)\lambda_1 V_1 - (\sigma_1 + \gamma_{C1} + \mu)C_1, \tag{2.7}$$

where τ_1 is the proportion moving to the infected class of strain 1 without first passing through here.

The carrier population of strain 2 is composed of a population infected with Neisseria meningitidis, but do not show any signs or symptoms even though they are infectious. This is generated by the effective contact rate λ_2, and decreased as a result of the progression of individuals to the infected population of strain 2 at rate σ_2. This population is also decreased by the recovery rate γ_{C2} and natural death rate μ. Therefore, the rate of change in the carrier population of strain 2 can be described by the following differential equation

$$\frac{dC_2}{dt} = \lambda_2(1-\tau_2)S + (1-\epsilon_2)\lambda_2 V_2 - (\sigma_2 + \gamma_{C2} + \mu)C_2, \tag{2.8}$$

where τ_2 is the proportion that moves to the infected class of strain 2 without first passing through the carrier population.

The infected population of strain 1 is a population with a fully blown infection of Streptococcus pneumoniae and shows signs and symptoms. This population is said to have

survived an average incubation period of 1–3 days. This is also generated by the effective contact rate λ_1 and carrier progression at rate σ_1. The population is decreased by the recovery rate γ_{I1}, disease-induced death rate δ, and natural death rate μ. Hence, the ODE governing the dynamics of the infected population of strain 1 is given by

$$\frac{dI_1}{dt} = \sigma_1 C_1 + \lambda_1 \tau_1 S + \lambda_1 V_2 - (\gamma_{I1} + \delta + \mu) I_1. \quad (2.9)$$

The infected population of strain 2 is a population with a fully blown infection from Neisseria meningitidis that exhibits signs and symptoms of infection. This population is said to have survived an average incubation period of 4 days. This is also generated by the force of infection λ_2 and the progression of the carrier at the rate σ_2. The population is decreased by the recovery rate γ_{I2}, disease-induced death rate δ, and natural death rate μ. It follows that the rate of change of the infected population of strain 2 is described by the ODE, given as

$$\frac{dI_2}{dt} = \sigma_2 C_2 + \lambda_2 \tau_2 S + \lambda_2 V_1 - (\gamma_{I2} + \delta + \mu) I_2. \quad (2.10)$$

The first recovered class, $R_1(t)$, is the population of individuals who have fully recovered from infection by either strain. This population increases because of the recovery of carriers at rates γ_{C1}, γ_{C2} and infections at rates γ_{I1}, γ_{I2}. They are decreased by the complication rate after a period $\wedge$ and the natural death rate μ. Thus, the rate of change of the fully recovered population is expressed as

$$\frac{dR_1}{dt} = \gamma_{C1} C_1 + \gamma_{C2} C_2 + \gamma_{I1} \rho_1 I_1 + \gamma_{I2} \rho_2 I_2 - (\wedge + \mu) R_1. \quad (2.11)$$

The second recovered class, $R_2(t)$, is the number of individuals who recovered from infection by either strain with complications owing to the sequelae of the delibitating effects among survivors, even after recovery. This population is also increased by the recovery rates of the infected populations γ_{I1}, γ_{I2}, and the complication rate $\wedge$ and decrease because of the natural death rate μ. Hence, the rate of change of the recovered with complication population is described by the ODE, given by

$$\frac{dR_2}{dt} = \gamma_{I1}(1 - \rho_1) I_1 + \gamma_{I2}(1 - \rho_2) I_2 + \wedge R_1 - \mu R_2. \quad (2.12)$$

We note that all parameters are assumed to be nonnegative in an epidemiological sense.

The model parameters and model state variables are shown in Tables 1 and 2.

Table 1. Description of model parameters [22,23].

Parameters	Description
α	Birth or recruitment rate into susceptible population
β	Transmission probability
δ	Disease-induced death rate
μ	Natural death rate
σ_1	Rate of progression from carrier of strain 1 to infected population of strain 1
σ_2	Rate of progression from carrier of strain 2 to infected population of strain 2
γ_{C1}	Recovery rate of carriers of strain 1
γ_{C2}	Recovery rate of carriers of strain 2
γ_{I1}	Recovery rate of infected with strain 1
γ_{I2}	Recovery rate of infected with strain 2
θ_1	Strain 1 vaccine uptake rate
θ_2	Strain 2 vaccine uptake rate
ϵ_1	Strain 1 vaccine efficacy
ϵ_2	Strain 2 Vaccine efficacy
ω_1	Vaccine waning of strain 1
ω_2	Vaccine waning of strain 2
τ_1	Proportion moving to I_1 without first passing through C_1
τ_2	Proportion moving to I_2 without first passing through C_2
$\wedge$	Complication rate after a period of time
ρ_1	Proportion moving to $R_1(t)$ from strain 1 without first passing through $R_2(t)$
ρ_2	Proportion moving to $R_1(t)$ from strain 2 without first passing through $R_2(t)$

Table 2. Description of the model state variables [22, 23].

Variables	Description
$S(t)$	Susceptible population who can contract both strains 1 and 2
$V_1(t)$	Vaccinated population with immunity to strain 1
$V_2(t)$	Vaccinated population with immunity to strain 2
$C_1(t)$	Carrier population of strain 1
$C_2(t)$	Carrier population of strain 2
$I_1(t)$	Infected population of strain 1
$I_2(t)$	Infected population of strain 2
$R_1(t)$	Fully recovered population from both strains 1 and 2
$R_2(t)$	Recovered with complications from both strains 1 and 2

2.1. Model assumptions

(1) Only two strains of bacterial meningitis were considered in this study.
(2) Every individual in the studied population is susceptible to one of the two strains at a given time.
(3) Individuals cannot be infected by more than one bacteria strain at the same time.
(4) The vaccines are only administered to the susceptible population.
(5) A vaccinated individual who loses immunity will return to the susceptible class with no vaccine protection.
(6) There is permanent immunity after full recovery.

2.2. Model equations

Following the descriptions given in Eqs (2.4)–(2.12) and the flow diagram of the two-strain bacterial meningitis model presented in Figure 2, the model governing the system of nine mutually exclusive ODEs for bacterial meningitis population dynamics is expressed as

$$\begin{aligned}
\frac{dS}{dt} &= \alpha + \omega_1 V_1 + \omega_2 V_2 - (\lambda_1 + \lambda_2 + \theta_1 + \theta_2 + \mu)S,\\
\frac{dV_1}{dt} &= \theta_1 S - (1-\epsilon_1)\lambda_1 V_1 - (\lambda_2 + \omega_1 + \mu)V_1,\\
\frac{dV_2}{dt} &= \theta_2 S - (1-\epsilon_2)\lambda_2 V_2 - (\lambda_1 + \omega_2 + \mu)V_2,\\
\frac{dC_1}{dt} &= \lambda_1(1-\tau_1)S + (1-\epsilon_1)\lambda_1 V_1 - (\sigma_1 + \gamma_{C1} + \mu)C_1,\\
\frac{dC_2}{dt} &= \lambda_2(1-\tau_2)S + (1-\epsilon_2)\lambda_2 V_2 - (\sigma_2 + \gamma_{C2} + \mu)C_2,\\
\frac{dI_1}{dt} &= \sigma_1 C_1 + \lambda_1\tau_1 S + \lambda_1 V_2 - (\gamma_{I1} + \delta + \mu)I_1,\\
\frac{dI_2}{dt} &= \sigma_2 C_2 + \lambda_2\tau_2 S + \lambda_2 V_1 - (\gamma_{I2} + \delta + \mu)I_2,\\
\frac{dR_1}{dt} &= \gamma_{C1}C_1 + \gamma_{C2}C_2 + \gamma_{I1}\rho_1 I_1 + \gamma_{I2}\rho_2 I_2 - (\wedge + \mu)R_1,\\
\frac{dR_2}{dt} &= \gamma_{I1}(1-\rho_1)I_1 + \gamma_{I2}(1-\rho_2)I_2 + \wedge R_1 - \mu R_2,
\end{aligned} \tag{2.13}$$

subject to the initial conditions:

$$\begin{aligned}
S(0) = S_0, \quad V_1(0) = V_{01}, \; V_2(0) = V_{02},\\
C_1(0) = C_{01}, \; C_2(0) = C_{02}, \; I_1(0) = I_{01},\\
I_2(0) = I_{02}, \quad R_1(0) = R_{01}, R_2(0) = R_{02}.
\end{aligned} \tag{2.14}$$

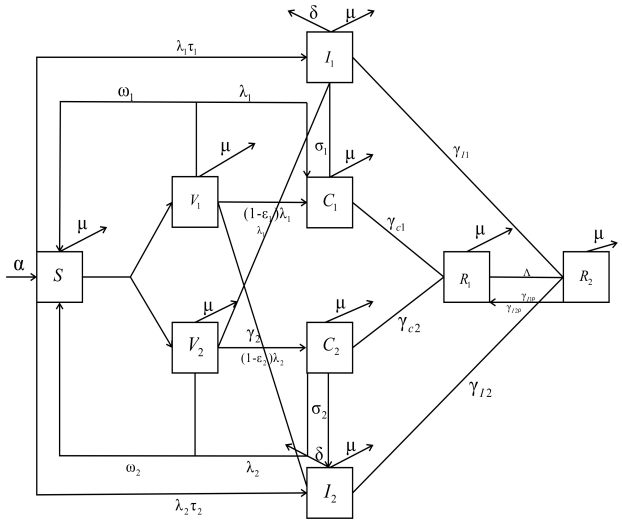

Figure 2. The schematic flow diagram of the transmission of two-strain bacterial meningitis.

3. The model analysis

3.1. Invariant region and positivity of solutions

Definition 3.1. A region within which the solutions to the model are uniformly bounded is defined as $\Omega \in \Re^9_+$.

From the total population in Eq (2.1), we have

$$\begin{aligned}
\frac{dN(t)}{dt} &= \frac{dS(t)}{dt} + \frac{dV_1(t)}{dt} + \frac{dV_2(t)}{dt} + \frac{dC_1(t)}{dt} + \frac{dC_2(t)}{dt}\\
&\quad + \frac{dI_1(t)}{dt} + \frac{dI_2(t)}{dtx} + \frac{dR_1(t)}{dt} + \frac{dR_2(t)}{dt}.
\end{aligned} \tag{3.1}$$

Substituting (2.13) into (3.1) and simplifying yields

$$\frac{dN(t)}{dt} = \alpha - \mu N - \delta I_1 - \delta I_2, \tag{3.2}$$

$$\frac{dN(t)}{dt} \leq \alpha - \mu N(t). \tag{3.3}$$

Integrating both sides of Eq (3.3), we have

$$-\frac{1}{\mu}\ln(\alpha - \mu N) \leq t + c, \tag{3.4}$$

where c is the constant of integration. Thus,

$$\ln(\alpha - \mu N) \geq -(\mu t + c), \tag{3.5}$$

$$(\alpha - \mu N) \geq k e^{-\mu t}, \tag{3.6}$$

where k is e^c.

Let $N(0) = N_0$, this implies

$$(\alpha - \mu N_0) \geq k. \tag{3.7}$$

From (3.6) and (3.7), we get

$$\begin{aligned} (\alpha - \mu N) &\geq (\alpha - \mu N_0)e^{-\mu t}, & (3.8)\\ N(t) &\leq \frac{\alpha}{\mu} - \frac{(\alpha - \mu N_0)}{\mu}e^{-\mu t}, & (3.9) \end{aligned}$$

So,

$$N(t) \rightarrow \frac{\alpha}{\mu} \text{ as } t \rightarrow \infty, \tag{3.10}$$

implies $N(t) \in [0, \frac{\alpha}{\mu}]$.

Therefore, the feasible set of solutions of the model equations enter and remain in the invariant region

$$\Omega = \{(S, V_1, V_2, C_1, C_2, I_1, I_2, R_1, R_2) \in \Re_+^9 : N(t) \leq \frac{\alpha}{\mu}\}. \tag{3.11}$$

Therefore, $N(t)$ is bounded; thus, the model is mathematically and epidemiologically well-posed because region Ω is positively invariant and attractive. Hence, it is sufficient to study the dynamics of model (2.13) in Ω.

Theorem 3.1. *The positivity theorem: Let*

$$\begin{aligned} \Omega =\{&(S, V_1, V_2, C_1, C_2, I_1, I_2, R_1, R_2) \in \Re_+^9 : S_0 > 0,\\ &V_{01} > 0, V_{02} > 0, C_{01} > 0, C_{02} > 0, I_{01} > 0,\\ &I_{02} > 0, R_{01} > 0, R_{02} > 0\}, \end{aligned}$$

then, the solutions $(S, V_1, V_2, C_1, C_2, I_1, I_2, R_1, R_2)$ *are positive for* $t \geq 0$.

Proof. Considering the first equation of the model

$$\begin{aligned} \frac{dS}{dt} &= \alpha + \omega_1 V_1 + \omega_2 V_2 - (\lambda_1 + \lambda_2 + \theta_1 + \theta_2 + \mu)S,\\ \frac{dS}{dt} &\geq -(\lambda_1 + \lambda_2 + \theta_1 + \theta_2 + \mu)S,\\ \int \frac{dS}{S} &\geq -\int (\lambda_1 + \lambda_2 + \theta_1 + \theta_2 + \mu)dt,\\ \ln S(t) &\geq -f(t) + c, \end{aligned}$$

where

$$f(t) = \int (\lambda_1 + \lambda_2 + \theta_1 + \theta_2 + \mu)dt$$

and c is the constant of integration. Hence,

$$S(t) \geq e^{(-f(t)+c)} = A_1 e^{-f(t)}, \tag{3.12}$$

where $A_1 = e^c$.

From Theorem 3.1, at $t = 0$, $S_0 > 0$ which implies $A_1 = e^c \geq 0$ since $S(0) \geq A_1$. Consequently,

$$S(t) \geq S_0 e^{-f(t)} \geq 0, \quad \forall t \geq 0.$$

Similarly, it can be shown that

$$\begin{aligned} V_1(t) &\geq V_{01}e^{-g(t)} \geq 0, & \forall t \geq 0,\\ V_2(t) &\geq V_{02}e^{-h(t)} \geq 0, & \forall t \geq 0,\\ C_1(t) &\geq C_{01}e^{-k_1 t} \geq 0, & \forall t \geq 0,\\ C_2(t) &\geq C_{02}e^{-k_2 t} \geq 0, & \forall t \geq 0,\\ I_1(t) &\geq I_{01}e^{-k_3 t} \geq 0, & \forall t \geq 0,\\ I_2(t) &\geq I_{02}e^{-k_4 t} \geq 0, & \forall t \geq 0,\\ R_1(t) &\geq R_{01}e^{-k_5 t} \geq 0, & \forall t \geq 0,\\ R_2(t) &\geq R_{02}e^{-\mu t} \geq 0, & \forall t \geq 0, \end{aligned} \tag{3.13}$$

where

$$g(t) = \int [(1 - \epsilon_1)\lambda_1 + \lambda_2 + \omega_1 + \mu]dt,$$

$$h(t) = \int [(1 - \epsilon_2)\lambda_2 + \lambda_1 + \omega_2 + \mu]dt,$$

$$k_1 = (\sigma_1 + \gamma_{C1} + \mu), \quad k_2 = (\sigma_2 + + \gamma_{C2} + \mu),$$

$$k_3 = (\gamma_{I1} + \delta + \mu), \quad k_4 = (\gamma_{I2} + \delta + \mu), \quad k_5 = (\wedge + \mu).$$

This completes the proof of the theorem. □

3.2. Existence of equilibria

For the developed model, four equilibrium points are identified when each compartment is in steady state. These are the disease-free equilibrium (DFE), endemic equilibrium and the boundary equilibrium points.

3.2.1. The DFE point

The DFE of the model is defined as $(S^*(t), V_1^*(t), V_2^*(t), 0, 0, 0, 0, 0, 0)$ satisfying

$$\begin{aligned} \frac{dS(t)}{dt} &= \frac{dV_1(t)}{dt} = \frac{dV_2(t)}{dt} = \frac{dC_1(t)}{dt} = \frac{dC_2(t)}{dt}\\ &= \frac{dI_1(t)}{dt} = \frac{dI_2(t)}{dt} = \frac{dR_1(t)}{dt} = \frac{dR_2(t)}{dt}\\ &= 0. \end{aligned}$$

Equating the system of equations in (2.13) to 0 and substituting

$$C_1 = C_2 = I_1 = I_2 = R_1 = R_2 = 0,$$

the DFE is obtained as

$$E_0 = \left(\frac{(\omega_1+\mu)(\omega_2+\mu)\alpha}{\chi\mu}, \frac{(\omega_2+\mu)\theta_1\alpha}{\chi\mu}, \frac{(\omega_1+\mu)\theta_2\alpha}{\chi\mu}, 0, 0, 0, 0, 0, 0\right), \tag{3.14}$$

where

$$\chi = \left(\mu^2 + \mu\,\omega_1 + \mu\,\omega_2 + \mu\,\theta_1 + \mu\,\theta_2 + \omega_1\omega_2 + \omega_1\theta_2 + \omega_2\theta_1\right). \tag{3.15}$$

3.2.2. Endemic equilibrium point

The edemic equilibrium point of the model is defined as

$$(S^*(t), V_1^*(t), V_2^*(t), C_1^*(t), C_2^*(t), I_1^*(t), I_2^*(t), R_1^*(t), R_2^*(t))$$

satisfying

$$\begin{aligned}\frac{dS(t)}{dt} &= \frac{dV_1(t)}{dt} = \frac{dV_2(t)}{dt} = \frac{dC_1(t)}{dt} = \frac{dC_2(t)}{dt}\\ &= \frac{dI_1(t)}{dt} = \frac{dI_2(t)}{dt} = \frac{dR_1(t)}{dt} = \frac{dR_2(t)}{dt}\\ &= 0.\end{aligned}$$

3.2.3. Boundary equilibrium points

Two boundary equilibrium points denoted by $\mathcal{E}_1$ and $\mathcal{E}_2$ are defined by

$$\mathcal{E}_1 = (S^*(t), V_1^*(t), V_2^*(t), C_1^*(t), 0, I_1^*(t), 0, R_1^*(t), R_2^*(t)), \tag{3.16}$$

where only strain 1 survives, and

$$\mathcal{E}_2 = (S^*(t), V_1^*(t), V_2^*(t), 0, C_2^*(t), 0, I_2^*(t), R_1^*(t), R_2^*(t)), \tag{3.17}$$

where only strain 2 survives.

Solving the system of equations for $\mathcal{E}_1$ results in

$$\begin{aligned} S^* &= \tfrac{(\lambda_1+b_7)[(1-\epsilon_1)\lambda_1+b_4]\alpha}{(1-\epsilon_1)\lambda_1{}^3+G_2\lambda_1{}^2+G_1\lambda_1+\mu\chi},\\ V_1^* &= \tfrac{\theta_1 S^*}{(1-\epsilon_1)\lambda_1+b_4},\\ V_2^* &= \tfrac{\theta_2 S^*}{\lambda_1+b_7},\\ C_1^* &= \tfrac{\lambda_1 S^*[\theta_1(1-\epsilon_1)+(1-\tau_1)((1-\epsilon_1)\lambda_1+b_4)]}{a_2((1-\epsilon_1)\lambda_1+b_4)},\\ I_1^* &= \tfrac{\lambda_1\tau_1 S^*+\sigma_1 C_1^*+\lambda_1 V_2^*}{a_1},\\ R_1^* &= \tfrac{\gamma_{I1}\rho_1 I_1^*+\gamma_{c1}C_1^*}{\wedge+\mu},\\ R_2^* &= \tfrac{\gamma_{I1}\left[(1-\rho_1)\mu+\wedge\right]I_1^*+\gamma_{C1}\wedge C_1^*}{\mu(\wedge+\mu)}, \end{aligned} \tag{3.18}$$

where

$$a_1 = \gamma_{I1}+\delta+\mu,\ a_2 = \sigma_1+\gamma_{C1}+\mu,\ b_4 = \omega_1+\mu,\ b_7 = \omega_2+\mu,$$

$$G_1 = [\chi - \omega_1(b_7+\theta_2)](1-\epsilon_1) + \mu\,b_4 - \omega_2\theta_1 + \chi,$$

$$G_2 = (1-\epsilon_1)(b_7+\theta_1+\theta_2+\mu) + b_4.$$

Substituting the state solutions in Eq (3.18) into the force of infection in Eq (2.2) yields the following cubic polynomial after some computation

$$K_1\lambda_1^{*3} + K_2\lambda_1^{*2} + K_3\lambda_1^* + K_4 = 0, \tag{3.19}$$

where

$$\begin{aligned}
K_1 &= (1-\epsilon_1)\left[(1-\tau_1)((\mu+\gamma_{I1})\sigma_1 + (\mu+\gamma_{c1})a_1) + a_2(\mu+\gamma_{I1})\tau_1\right],\\
K_2 &= (1-\tau_1)\left[(1-\epsilon_1)b_7 + b_4\right]\left[\sigma_1(\mu+\gamma_{I1}) + a_1(\mu+\gamma_{c1})\right]\\
&\quad + a_1\theta_1(1-\epsilon_1)(\mu+\gamma_{c1}) + (1-\epsilon_1)(\mu+\gamma_{I1})\left[a_2(\tau_1 b_7\right.\\
&\quad \left.+\theta_2) + \sigma_1\theta_1\right] - \beta\mu(1-\epsilon_1)(1-\tau_1)(\eta a_1+\sigma_1)\\
&\quad + a_2 b_4\tau_1(\mu+\gamma_{I1}) - \mu a_2(1-\epsilon_1)(\beta\tau_1 - a_1),\\
K_3 &= b_7\sigma_1(\mu+\gamma_{I1})\left[(1-\tau_1)b_4 + (1-\epsilon_1)\theta_1\right]\\
&\quad + a_1 b_7\left[(1-\tau_1)b_4 + (1-\epsilon_1)\theta_1\right](\mu+\gamma_{c1})\\
&\quad + a_2(b_7\tau_1+\theta_2)\left[b_4(\mu+\gamma_{I1}) - \mu\beta(1-\epsilon_1)\right]\\
&\quad + \mu a_1 a_2(1-\epsilon_1)(\theta_2+b_7) + \mu a_1 a_2(\theta_1+b_4)\\
&\quad - \beta\mu a_2 b_4\tau_1 - \mu\beta(\eta a_1+\sigma_1)((1-\tau_1)(1-\epsilon_1)b_7\\
&\quad + (1-\tau_1)b_4 + (1-\epsilon_1)\theta_1),\\
K_4 &= -\beta\mu(-b_4 b_7(-1+\tau_1)(\eta a_1+\sigma_1) + b_7\theta_1(1-\epsilon_1)(\eta a_1+\sigma_1)\\
&\quad + b_4(b_7\tau_1+\theta_2)a_2) + \mu a_1 a_2\chi,\\
&= -\beta\mu\left(b_7(\eta a_1+\sigma_1)((1-\tau_1)b_4 + (1-\epsilon_1)\theta_1) + b_4(b_7\tau_1+\theta_2)a_2\right)\\
&\quad + \mu a_1 a_2\chi,\\
&= \left(1 - \frac{\beta\left(b_7(\eta a_1+\sigma_1)((1-\tau_1)b_4 + (1-\epsilon_1)\theta_1) + b_4(b_7\tau_1+\theta_2)a_2\right)}{a_1 a_2\chi}\right)\\
&\quad \cdot \mu a_1 a_2\chi\\
&= \mu a_1 a_2\chi(1-\mathcal{R}_{01}),
\end{aligned}$$

and $\mathcal{R}_{01}$ is the basic reproduction number related to strain 1 as later defined in Eq (3.29).

Solving the system of equations for $\mathcal{E}_2$ results in

$$\begin{aligned} S^* &= \tfrac{(\lambda_2+b_4)[(1-\epsilon_2)\lambda_2+b_7]\alpha}{(1-\epsilon_2)\lambda_2{}^3+G_4\lambda_2{}^2+G_3\lambda_2+\mu\chi},\\ V_1^* &= \tfrac{\theta_1 S^*}{\lambda_2+b_4},\\ V_2^* &= \tfrac{\theta_2 S^*}{(1-\epsilon_2)\lambda_2+b_7},\\ C_2^* &= \tfrac{\lambda_2 S^*[\theta_2(1-\epsilon_2)+(1-\tau_2)((1-\epsilon_2)\lambda_2+b_7)]}{a_4((1-\epsilon_2)\lambda_2+b_7)},\\ I_2^* &= \tfrac{\lambda_2\tau_2 S^*+\sigma_2 C_2^*+\lambda_2 V_1^*}{a_3},\\ R_1^* &= \tfrac{\gamma_{I2}\rho_2 I_2^*+\gamma_{c2}C_2^*}{\wedge+\mu},\\ R_2^* &= \tfrac{\gamma_{I2}\left[(1-\rho_2)\mu+\wedge\right]I_2^*+\gamma_{C2}\wedge C_2^*}{\mu(\wedge+\mu)}, \end{aligned} \tag{3.20}$$

where

$$a_3 = \gamma_{I2}+\delta+\mu,\ \ a_4 = \sigma_2+\gamma_{C2}+\mu,$$

$$G_3 = [\chi - \omega_2 (b_4 + \theta_1)] (1 - \epsilon_2) + \mu b_7 - \omega_1 \theta_2 + \chi,$$

$$G_4 = (1 - \epsilon_2) (b_4 + \theta_1 + \theta_2 + \mu) + b_7.$$

Substituting the state solutions in Eq (3.20) into the force of infection in Eq (2.3) also yields the following cubic polynomial after some computations

$$K_5 \lambda_2^{*3} + K_6 \lambda_2^{*2} + K_7 \lambda_2^{*} + K_8 = 0, \tag{3.21}$$

where

$$\begin{aligned}
K_5 =& (1 - \epsilon_2) [(1 - \tau_2) ((\mu + \gamma_{I2}) \sigma_2 + (\mu + \gamma_{c2}) a_3) + a_4 (\mu + \gamma_{I2}) \tau_2],\\
K_6 =& (1 - \tau_2) [(1 - \epsilon_2) b_4 + b_7][\sigma_2 (\mu + \gamma_{I2}) + a_3 (\mu + \gamma_{c2})]\\
&+ a_3 \theta_2 (1 - \epsilon_2) (\mu + \gamma_{c2}) + (1 - \epsilon_2) (\mu + \gamma_{I2}) [a_4 (\tau_2 b_4 + \theta_1) + \sigma_2 \theta_2]\\
&- \beta \mu (1 - \epsilon_2) (1 - \tau_2) (\eta a_3 + \sigma_1)\\
&- \mu a_4 (1 - \epsilon_2) (\beta \tau_2 - a_3) + a_4 b_7 \tau_2 (\mu + \gamma_{I2}),\\
K_7 =& b_4 \sigma_2 (\mu + \gamma_{I2}) [(1 - \tau_2) b_7 + (1 - \epsilon_2) \theta_2] + a_3 b_4 [(1 - \tau_2) b_7\\
&+ (1 - \epsilon_2) \theta_2] (\mu + \gamma_{c2}) + a_4 (b_4 \tau_2 + \theta_1) [b_7 (\mu + \gamma_{I2}) - \mu \beta (1 - \epsilon_2)]\\
&+ \mu a_3 a_4 (1 - \epsilon_2) (\theta_1 + b_4) + \mu a_3 a_4 (\theta_2 + b_7) - \beta \mu a_4 b_7 \tau_2\\
&- \mu \beta (\eta a_3 + \sigma_2) ((1 - \tau_2) (1 - \epsilon_2) b_4 + (1 - \tau_2) b_7 + (1 - \epsilon_2) \theta_2),\\
K_8 =& - \beta \mu (-b_4 b_7 (-1 + \tau_2) (\eta a_3 + \sigma_2) + b_7 \theta_2 (1 - \epsilon_2) (\eta a_3 + \sigma_2)\\
&+ b_7 (b_4 \tau_2 + \theta_1) a_4) + \mu a_3 a_4 \chi,\\
=& - \beta \mu (b_4 (\eta a_3 + \sigma_2) ((1 - \tau_2) b_7 + (1 - \epsilon_2) \theta_2)\\
&+ b_7 (b_4 \tau_2 + \theta_1) a_4) + \mu a_3 a_4 \chi\\
=& \mu a_3 a_4 \chi (1 - \mathcal{R}_{02}),
\end{aligned}$$

and $\mathcal{R}_{02}$ is the basic reproduction number relating to strain 2 as later defined in Eq (3.30).

3.3. Stability analysis of the DFE

3.3.1. The basic reproduction number

The basic reproduction number is defined as the average number of secondary infections caused by a single infectious individual in a completely susceptible population. It helps forecast the transmission potential of a disease. According to the principle of the next generation matrix, the basic reproduction number is the spectral radius of the next generation matrix $\mathcal{F}\mathcal{V}^{-1}$ in model (2.13). Following [27,28], the basic reproduction number associated with model (2.13) is derived as follows

$$\begin{pmatrix} \frac{dC_1}{dt} \\ \frac{dI_1}{dt} \\ \frac{dC_2}{dt} \\ \frac{dI_2}{dt} \end{pmatrix} = f_i - v_i,$$

with

$$f_i = \begin{pmatrix} \lambda_1(1 - \tau_1)S + (1 - \epsilon_1)\lambda_1 V_1 \\ \lambda_1 \tau_1 S + \lambda_1 V_2 \\ \lambda_2(1 - \tau_2)S + (1 - \epsilon_2)\lambda_2 V_2 \\ \lambda_2 \tau_2 S + \lambda_2 V_1 \end{pmatrix} \tag{3.22}$$

and

$$v_i = \begin{pmatrix} (\sigma_1 + \gamma_{C1} + \mu)C_1 \\ (\gamma_{I1} + \delta + \mu)I_1 - \sigma_1 C_1 \\ (\sigma_2 + \gamma_{C2} + \mu)C_2 \\ (\gamma_{I2} + \delta + \mu)I_2 - \sigma_2 C_2 \end{pmatrix}, \tag{3.23}$$

where, f_i is the rate of appearance of new infection(s) in compartment i, v_i represents the rate of transfer of individuals into compartment i, with $i \in [1, 2]$.
The Jacobian of f_i at E_0 is given as

$$\mathcal{F} = \begin{pmatrix} \frac{\eta\beta b_7[\theta_1(1-\epsilon_1)+(1-\tau_1)b_4]}{\chi} & \frac{\beta b_7[\theta_1(1-\epsilon_1)+(1-\tau_1)b_4]}{\chi} & 0 & 0 \\ \frac{\eta\beta b_4(b_7\tau_1+\theta_2)}{\chi} & \frac{\beta b_4(b_7\tau_1+\theta_2)}{\chi} & 0 & 0 \\ 0 & 0 & \frac{\eta\beta b_4[\theta_2(1-\epsilon_2)+(1-\tau_2)b_7]}{\chi} & \frac{\beta b_4[\theta_2(1-\epsilon_2)+(1-\tau_2)b_7]}{\chi} \\ 0 & 0 & \frac{\eta\beta b_7(b_4\tau_2+\theta_1)}{\chi} & \frac{\beta b_7(b_4\tau_2+\theta_1)}{\chi} \end{pmatrix} \tag{3.24}$$

and that of v_i at E_0 is given as

$$\mathcal{V} = \begin{pmatrix} \sigma_1 + \gamma_{C1} + \mu & 0 & 0 & 0 \\ -\sigma_1 & \gamma_{I1} + \delta + \mu & 0 & 0 \\ 0 & 0 & \sigma_2 + \gamma_{C2} + \mu & 0 \\ 0 & 0 & -\sigma_2 & \gamma_{I2} + \delta + \mu \end{pmatrix} \tag{3.25}$$

with

$$\mathcal{V}^{-1} = \begin{pmatrix} \frac{1}{\sigma_1+\gamma_{C1}+\mu} & 0 & 0 & 0 \\ \frac{\sigma_1}{(\sigma_1+\gamma_{C1}+\mu)(\gamma_{I1}+\delta+\mu)} & \frac{1}{\gamma_{I1}+\delta+\mu} & 0 & 0 \\ 0 & 0 & \frac{1}{\sigma_2+\gamma_{C2}+\mu} & 0 \\ 0 & 0 & \frac{\sigma_2}{(\sigma_2+\gamma_{C2}+\mu)(\gamma_{I2}+\delta+\mu)} & \frac{1}{\gamma_{I2}+\delta+\mu} \end{pmatrix}. \tag{3.26}$$

Thus, the next generation matrix is calculated as

$$\begin{aligned}
G =& \mathcal{F}\mathcal{V}^{-1}\\
=& \begin{pmatrix} \frac{\eta\beta b_7 b_1(\eta a_1+\sigma_1)}{\chi a_1 a_2} & \frac{\beta b_7 b_1}{\chi a_1} & 0 & 0 \\ \frac{\eta\beta b_4(b_7\tau_1+\theta_2)(\eta a_1+\sigma_1)}{\chi a_1 a_2} & \frac{\beta b_4(b_7\tau_1+\theta_2)}{\chi a_1} & 0 & 0 \\ 0 & 0 & \frac{\beta b_4 b_2(\eta a_3+\sigma_2)}{\chi a_3 a_4} & \frac{\beta b_4 b_2}{\chi a_3} \\ 0 & 0 & \frac{\beta b_7(b_4\tau_2+\theta_1)(\eta a_3+\sigma_2)}{\chi a_3 a_4} & \frac{\beta b_7(b_4\tau_2+\theta_1)}{\chi a_3} \end{pmatrix},
\end{aligned} \tag{3.27}$$

where,

$$b_1 = \theta_1(1 - \epsilon_1) + (1 - \tau_1)b_4, \;\; b_2 = \theta_2(1 - \epsilon_2) + (1 - \tau_2)b_7.$$

The eigenvalues of the matrix G in Eq (3.27) are

$$\lambda^T = \begin{pmatrix} 0 \\ 0 \\ \frac{\beta\,[b_7(\eta\,a_1+\sigma_1)(b_4(1-\tau_1)+\theta_1(1-\epsilon_1))+a_2b_4(b_7\tau_1+\theta_2)]}{a_1a_2\chi} \\ \frac{\beta\,[b_4(\eta\,a_3+\sigma_2)(b_7(1-\tau_2)+\theta_2(1-\epsilon_2))+a_4b_7(b_4\tau_2+\theta_1)]}{a_3a_4\chi} \end{pmatrix}. \quad (3.28)$$

Consequently, the basic reproduction number, which is the spectral radius of G is given as $\mathcal{R}_0 = \max\{\mathcal{R}_{01}, \mathcal{R}_{02}\}$, with

$$\mathcal{R}_{01} = \frac{\beta\,[b_7\,(\eta\,a_1+\sigma_1)\,(b_4\,(1-\tau_1)+\theta_1\,(1-\epsilon_1))+a_2b_4\,(b_7\tau_1+\theta_2)]}{a_1a_2\chi}, \quad (3.29)$$

$$\mathcal{R}_{02} = \frac{\beta\,[b_4\,(\eta\,a_3+\sigma_2)\,(b_7\,(1-\tau_2)+\theta_2\,(1-\epsilon_2))+a_4b_7\,(b_4\tau_2+\theta_1)]}{a_3a_4\chi}, \quad (3.30)$$

representing the basic reproduction numbers related to strain 1 and 2, respectively.

The expression $\mathcal{R}_{01}$ in Eq (3.29) provides the expected number of newly infected individuals that would arise as a result of introducing a single case of strain 1 into a completely susceptible population [29]. Similarly, $\mathcal{R}_{02}$, given by Eq (3.30), yields the expected number of newly infected individuals that would arise if a single case of strain 2 is introduced into a completely susceptible population.

3.3.2. Local stability of the DFE

Theorem 3.2. *The DFE is locally asymptotically stable if* $\mathcal{R}_0 < 1$ *and unstable if* $\mathcal{R}_0 > 1$.

Using Theorem 3.2, the result in Lemma 3.1 follows immediately based on the expressions of $\mathcal{R}_{01}, \mathcal{R}_{02}$.

Lemma 3.1. *The DFE of the two-strain bacterial meningitis model in* (2.13) *is locally asymptotically stable if both* $\mathcal{R}_{01}, \mathcal{R}_{02} < 1$ *and unstable if* $\mathcal{R}_{01}, \mathcal{R}_{02} > 1$.

Definition 3.2. The DFE of model (2.13) is said to be locally stable if each eigenvalue of the associated Jacobian matrix is negative.

Following Definition 3.2, the Jacobian matrix, J evaluated at E_0 is given as

$$J = \begin{pmatrix} -b_3 & \omega_1 & \omega_2 & -\frac{\beta\eta b_4b_7}{\chi} & -\frac{\beta\eta b_1b_7}{\chi} & -\frac{\beta b_4b_7}{\chi} & -\frac{\beta b_4b_7}{\chi} & 0 & 0 \\ \theta_1 & -b_4 & 0 & -\frac{\beta\eta\theta_1(1-\epsilon_1)b_7}{\chi} & -\frac{\beta\eta b_7\theta_1}{\chi} & -\frac{\beta\theta_1(1-\epsilon_1)b_7}{\chi} & -\frac{\beta b_7\theta_1}{\chi} & 0 & 0 \\ \theta_2 & 0 & -b_7 & -\frac{\beta\eta b_4\theta_2}{\chi} & -\frac{\beta\eta\theta_2(1-\epsilon_2)b_4}{\chi} & -\frac{\beta b_4\theta_2}{\chi} & -\frac{\beta\theta_2(1-\epsilon_2)b_4}{\chi} & 0 & 0 \\ 0 & 0 & 0 & \frac{\beta\eta b_1b_7}{\chi} - a_2 & 0 & \frac{\beta b_1b_7}{\chi} & 0 & 0 & 0 \\ 0 & 0 & 0 & 0 & \frac{\beta\eta b_2b_4}{\chi} - a_4 & 0 & \frac{\beta b_2b_4}{\chi} & 0 & 0 \\ 0 & 0 & 0 & \frac{\beta\eta b_4b_6}{\chi} + \sigma_1 & 0 & \frac{\beta b_4b_6}{\chi} - a_1 & 0 & 0 & 0 \\ 0 & 0 & 0 & 0 & \frac{\beta\eta b_7b_5}{\chi} + \sigma_2 & 0 & \frac{\beta b_7b_5}{\chi} - a_3 & 0 & 0 \\ 0 & 0 & 0 & \gamma_{C1} & \gamma_{C2} & \gamma_{I1}\rho_1 & \gamma_{I2}\rho_2 & -(\wedge+\mu) & 0 \\ 0 & 0 & 0 & 0 & 0 & \gamma_{I1}(1-\rho_1) & \gamma_{I2}(1-\rho_2) & \wedge & -\mu \end{pmatrix} \quad (3.31)$$

where

$$b_3 = \theta_1 + \theta_2 + \mu, \;\; b_5 = b_4\tau_2 + \theta_1, \;\; b_6 = b_7\tau_1 + \theta_2.$$

The eigenvalues of the Jacobian matrix, J are

$$\lambda_{1,2} = -\frac{(a_1+a_2)\chi - \beta\,\eta\,b_1b_7 - \beta\,b_4b_6 \pm \sqrt{W_1}}{2\chi},$$
$$\lambda_{3,4} = -\frac{(a_3+a_4)\chi - \beta\,\eta\,b_2b_4 - \beta\,b_5b_7 \pm \sqrt{W_2}}{2\chi},$$
$$\lambda_5 = -\mu, \;\; \lambda_6 = -(\wedge+\mu),$$

where

$$W_1 = \beta^2(\eta\,b_1b_7 + b_4b_6)^2 + 2\chi\beta\,\eta\,b_1b_7(a_1-a_2) - 2\chi\beta\,b_4b_6(a_1-a_2) + 4\chi\beta\,b_1b_7\sigma_1 + \chi^2(a_1-a_2)^2$$

and

$$W_2 = \beta^2(\eta\,b_2b_4 + b_5b_7)^2 + 2\chi\beta\,\eta\,b_2b_4(a_3-a_4) - 2\chi\beta\,b_5b_7(a_3-a_4) + 4\chi\beta\,b_2b_4\sigma_2 + \chi^2(a_3-a_4)^2.$$

The remaining three eigenvalues of J are obtained as the roots of the following polynomial

$$c_1\lambda^3 + c_2\lambda^2 + c_3\lambda + c_4 \quad (3.32)$$

where,

$c_1 = 1,$

$c_2 = b_3 + b_4 + b_7,$

$c_3 = b_4b_7 + b_3(b_4+b_7) - \omega_1\theta_1 - \omega_2\theta_2 = \chi + \mu(b_3+b_4+\omega_2),$

$c_4 = b_3b_4b_7 - b_4\omega_2\theta_2 - b_7\omega_1\theta_1 = \chi\mu.$

Applying the Routh-Hurwitz criteria to cubic polynomial in Eq (3.32).

Because all the parameters of model (2.13) are positive, it is clear that the condition of stability is established with $c_1 > 0$, $c_2 > 0$, $c_3 > 0$ and $c_4 > 0$.

3.3.3. Global asymptotic stability of the DFE

The global asymptotic stability of the model in (2.13) is investigated by following [29, 30]. The model is denoted by

$$\begin{cases} \frac{dX}{dt} = F(X,Y), \\ \frac{dY}{dt} = G(X,Y), \end{cases} \tag{3.33}$$

where $X = (S, V_1, V_2, R_1, R_2)$ denotes the right-hand side of the uninfected population with $C_1 = C_2 = I_1 = I_2 = 0$ and $Y = (C_1, C_2, I_1, I_2)$ denotes the right-hand side of the infected population.

Theorem 3.3. *The DFE is said to be globally asymptotically stable in* Ω *if* $\mathcal{R}_{01}, \mathcal{R}_{02} < 1$ *and the following two conditions hold:*

C1: For $\frac{dX}{dt} = F(X, 0)$*,* E_0 *is globally asymptotically stable.*
C2: $G(X,Y) = J\,[G(X^*, 0)]\,Y - \hat{G}(X,Y)$,
$\hat{G}(X,Y) \geq 0, \ \ \forall\ (X,Y) \in \Omega,$

where

$$(X^*, 0) = E_0 = \left(\frac{\alpha b_4 b_7}{\mu\chi}, \frac{\alpha\theta_1 b_7}{\mu\chi}, \frac{\alpha\theta_2 b_4}{\mu\chi}, 0, 0, 0, 0, 0, 0\right),$$

$J\,[G(X^*, 0)]$ *is the Jacobian of* $G(X,Y)$ *obtained with respect to* $(C_1,\ C_2,\ I_1,\ I_2)$ *and evaluated at* $(X^*, 0)$*.*

Proof. **C1:** From the model, it follows that

$$F(X,0) = \begin{pmatrix} \alpha + \omega_1 V_1 + \omega_2 V_2 - (\theta_1 + \theta_2 + \mu)S \\ \theta_1 S - b_4 V_1 \\ \theta_2 S - b_7 V_2 \\ -(\wedge + \mu) R_1 \\ \wedge R_1 - \mu R_2 \end{pmatrix}. \tag{3.34}$$

From Eq (3.34), it is clear that

$$\begin{aligned} E_0 &= (S, V_1, V_2, C_1, C_2, I_1, I_2, R_1, R_2) \\ &= \left(\frac{\alpha b_4 b_7}{\mu\chi}, \frac{\alpha\theta_1 b_7}{\mu\chi}, \frac{\alpha\theta_2 b_4}{\mu\chi}, 0, 0, 0, 0, 0, 0\right). \end{aligned}$$

This can be verified using the method of integrating factors. From Eq (3.34), we have

$$\frac{dV_1}{dt} + b_4 V_1 = \theta_1 S. \tag{3.35}$$

The integrating factor is given as

$$e^{\int b_4 dt} = e^{b_4 t}.$$

Multiplying Eq (3.35) through by the integrating factor yields

$$e^{b_4 t}\left(\frac{dV_1}{dt} + b_4 V_1\right) = (\theta_1 S)\, e^{b_4 t},$$
$$\int \frac{d}{dt}\left(V_1 e^{b_4 t}\right) dt = \theta_1 \int S\, e^{b_4 t} dt.$$

Let

$$I = \int S\, e^{b_4 t} dt.$$

Integrating by parts, we have

$$u = S \implies du = S' dt$$

and

$$dv = e^{b_4 t} \implies v = \frac{e^{b_4 t}}{b_4}.$$

So,

$$I = \frac{S\, e^{b_4 t}}{b_4} - \frac{1}{b_4}\int S' e^{b_4 t} dt$$

implying that

$$V_1 e^{b_4 t} = \theta_1 \left[\frac{S\, e^{b_4 t}}{b_4} - \frac{1}{b_4}\int S' e^{b_4 t} dt\right].$$

Therefore,

$$V_1 = \frac{\theta_1 S}{b_4} - \frac{\theta_1}{b_4 e^{b_4 t}}\int S' e^{b_4 t} dt. \tag{3.36}$$

From Eq (3.36), $V_1 \to \frac{\theta_1 S}{b_4}$ as $t \to \infty$.

Similarly, we can deduce from Eq (3.34) that, $V_2 \to \frac{\theta_2 S}{b_7}$ as $t \to \infty$. Furthermore, from Eq (3.34), we have

$$\frac{dS}{dt} = \alpha + \omega_1 V_1 + \omega_2 V_2 - (\theta_1 + \theta_2 + \mu)S. \tag{3.37}$$

Since $V_1 \to \frac{\theta_1 S}{b_4}$ and $V_2 \to \frac{\theta_2 S}{b_7}$, Eq (3.37) is rewritten as

$$\frac{dS}{dt} = \alpha + \frac{\omega_1\theta_1 S}{b_4} + \frac{\omega_2\theta_2 S}{b_7} - (\theta_1 + \theta_2 + \mu)S, \tag{3.38}$$
$$\frac{dS}{dt} + \frac{\mu\chi}{b_4 b_7} S = \alpha. \tag{3.39}$$

The integrating factor of Eq (3.39) is given as

$$e^{\int \frac{\mu\chi}{b_4 b_7} dt} = e^{\frac{\mu\chi}{b_4 b_7} t}.$$

Multiplying Eq (3.39) through by the integrating factor gives

$$e^{\frac{\mu\chi}{b_4 b_7} t}\left(\frac{dS}{dt} + \frac{\mu\chi}{b_4 b_7} S\right) = \alpha e^{\frac{\mu\chi}{b_4 b_7} t},$$

$$\int \frac{d}{dt}\left(S e^{\frac{\mu\chi}{b_4 b_7}t}\right)dt = \int \alpha e^{\frac{\mu\chi}{b_4 b_7}t}dt,$$
$$S e^{\frac{\mu\chi}{b_4 b_7}t} = \frac{\alpha b_4 b_7}{\mu\chi} e^{\frac{\mu\chi}{b_4 b_7}t} + c,$$

where c is the constant of integration. Therefore,

$$S = \frac{\alpha b_4 b_7}{\mu\chi} + Ce^{-\frac{\mu\chi}{b_4 b_7}t}. \tag{3.40}$$

From Eq (3.40), $S \to \frac{\alpha b_4 b_7}{\mu\chi}$ as $t \to \infty$; and this implies the global convergence of Eq (3.34) in Ω.

C2: $G(X, Y)$ is given as

$$G(X,Y) = \begin{bmatrix} \lambda_1(1-\tau_1)S + (1-\epsilon_1)\lambda_1 V_1 - a_2 C_1 \\ \lambda_2(1-\tau_2)S + (1-\epsilon_2)\lambda_2 V_2 - a_4 C_2 \\ \sigma_1 C_1 + \lambda_1\tau_1 S + \lambda_1 V_2 - a_1 I_1 \\ \sigma_2 C_2 + \lambda_2\tau_2 S + \lambda_2 V_1 - a_3 I_2 \end{bmatrix}, \tag{3.41}$$

where λ_1 and λ_2 are the forces of infection defined in Eqs (2.2) and (2.3).

By the condition in C2 with Eqs (3.41) and (3.43), $\hat{G}(X, Y)$ is given by

$$\begin{pmatrix} \frac{\beta(\eta C_1 + I_1)\left[(1-\epsilon_1)V_1^* + (1-\tau_1)S^*\right]}{N^*}\left(1 - \frac{(1-\epsilon_1)V_1 + (1-\tau_1)S}{N}\frac{N^*}{(1-\epsilon_1)V_1^* + (1-\tau_1)S^*}\right) \\ \frac{\beta(\eta C_2 + I_2)\left[(1-\epsilon_2)V_2^* + (1-\tau_2)S^*\right]}{N^*}\left(1 - \frac{(1-\epsilon_2)V_2 + (1-\tau_2)S}{N}\frac{N^*}{(1-\epsilon_2)V_2^* + (1-\tau_2)S^*}\right) \\ \frac{\beta(\eta C_1 + I_1)\left(\tau_1 S^* + V_2^*\right)}{N^*}\left(1 - \frac{(\tau_1 S + V_2)}{N}\frac{N^*}{(\tau_1 S^* + V_2^*)}\right) \\ \frac{\beta(\eta C_2 + I_2)\left(\tau_2 S^* + V_1^*\right)}{N^*}\left(1 - \frac{(\tau_2 S + V_1)}{N}\frac{N^*}{(\tau_2 S^* + V_1^*)}\right) \end{pmatrix}. \tag{3.42}$$

The Jacobian matrix of $G(X, Y)$, $J\left[G(X^*, 0)\right]$ is given as

$$\begin{pmatrix} \frac{\beta\eta\left[(1-\epsilon_1)V_1^* + (1-\tau_1)S^*\right] - a_2 N^*}{N^*} & 0 & \frac{\beta\left[(1-\epsilon_1)V_1^* + (1-\tau_1)S^*\right]}{N^*} & 0 \\ 0 & \frac{\beta\eta\left[(1-\epsilon_2)V_2^* + (1-\tau_2)S^*\right] - a_4 N^*}{N^*} & 0 & \frac{\beta\left[(1-\epsilon_2)V_2^* + (1-\tau_2)S^*\right]}{N^*} \\ \frac{\beta\eta\left(\tau_1 S^* + V_2^*\right) + \sigma_1 N^*}{N^*} & 0 & \frac{\beta\left(\tau_1 S^* + V_2^*\right) - a_1 N^*}{N^*} & 0 \\ 0 & \frac{\beta\eta\left(\tau_2 S^* + V_1^*\right) + \sigma_2 N^*}{N^*} & 0 & \frac{\beta\left(\tau_2 S^* + V_1^*\right) - a_3 N^*}{N^*} \end{pmatrix}. \tag{3.43}$$

Since

$$S^* = \frac{\alpha b_4 b_7}{\mu\chi}, \quad V_1^* = \frac{\alpha\theta_1 b_7}{\mu\chi}, \quad V_2^* = \frac{\alpha\theta_2 b_4}{\mu\chi} \text{ and } N^* = \frac{\alpha}{\mu},$$

we have that $S \le S^*$, $V_1 \le V_1^*$ and $V_2 \le V_2^*$. Thus, it follows that $S \le N$, $V_1 \le N$ and $V_2 \le N$ in Ω. Therefore, if the total population is at the equilibrium level, we have

$$\left(1 - \frac{(1-\epsilon_1)V_1 + (1-\tau_1)S}{N}\frac{N^*}{(1-\epsilon_1)V_1^* + (1-\tau_1)S^*}\right) > 0,$$

$$\left(1 - \frac{(1-\epsilon_2)V_2 + (1-\tau_2)S}{N}\frac{N^*}{(1-\epsilon_2)V_2^* + (1-\tau_2)S^*}\right) > 0,$$

$$\left(1 - \frac{(\tau_1 S + V_2)}{N}\frac{N^*}{(\tau_1 S^* + V_2^*)}\right) > 0$$

and

$$\left(1 - \frac{(\tau_2 S + V_1)}{N}\frac{N^*}{(\tau_2 S^* + V_1^*)}\right) > 0;$$

thus, $\hat{G}(X, Y) \ge 0$. Hence, it follows from Theorem 3.3 that the DFE, $E_0 = (X^*, 0)$ is globally asymptotically stable. □

3.4. Model parameter estimation and initial conditions

3.4.1. Initial conditions

The base year used in the simulations is 2017. As the disease is endemic to the northern part of Ghana, the total population of the northern part as of 2017, was 4953293 [31]; thus, the initial total population, $N(0) = 4953293$. Since the outbreak that year was due to the Neisseria meningitidis strain, the initially infected individuals of strain 2 were considered, $I_2(0) = 69$, which is the same number reported in data. We assumed $I_1(0) = 153$. According to a literature review, Streptococcus pneumoniae is found in the nose and throat of 20–40% of people, whereas Neisseria meningitidis is found in 1–10% of these people without causing any symptoms of illness. Thus, taking 140% and 110% of $I_1(0)$ and $I_2(0)$, respectively gives $C_1(0) = 214$ and $C_2(0) = 76$. We assumed

$$V_1(0) = V_2(0) = R_1(0) = R_2(0) = 0,$$

so the initial susceptible is

$$\begin{aligned} S(0) &= N(0) - V_1(0) - V_2(0) - C_1(0) - C_2(0) \\ &\quad - I_1(0) - I_2(0) - R_1(0) - R_2(0) \\ &= 4952781. \end{aligned}$$

3.4.2. Parameter values

(1) Natural death rate (μ): The average lifespan in Ghana is 64.17 years. Therefore,

$$\mu = \frac{1}{64.17 \times 365} = 4.269 \times 10^{-5}$$

per day.

(2) Birth or recruitment rate (α): The limiting total human population in the absence of the disease is assumed to be $\frac{\alpha}{\mu} = 4953293$, so $\alpha = 211$ per day.

(3) Disease-induced death rate (δ): The mortality rate due to bacterial meningitis disease in Ghana is 36–50%. By taking the average of 43%, we obtain that $\delta = 0.43$.

(4) Progression rates (σ_1, σ_2): The average incubation period for Streptococcus pneumonaie is 1–3 days while Neisseria meningitidis is 4 days. Thus,

$$\sigma_1 = \frac{1}{2} = 0.5 \text{ and } \sigma_2 = \frac{1}{4} = 0.25$$

(5) Vaccine waning rates (ω_1, ω_2): It takes 5 years for the pneumococcal conjugate vaccines to wane while that of the meningococcal conjugate vaccines is 3–5 years. Therefore,

$$\omega_1 = \frac{1}{5 \times 365} = 5.47 \times 10^{-4}$$

per day and

$$\omega_2 = \frac{1}{4 \times 365} = 6.8 \times 10^{-4}$$

per day.

(6) Recovery rates (γ_{C1}, γ_{I1}): The period of infection of the disease is 1-2 weeks with hospitalization and right treatment, so taking the average, we have 8 days. Thus,

$$\gamma_{I1} = \frac{1}{8} = 0.125.$$

For individuals exposed to the disease, prophylaxis is administered and it has been shown to be effective for 1-2 weeks of follow-up [32]. Thus,

$$\gamma_{C1} = \frac{1}{7} = 0.143.$$

(7) Complication rate ($\wedge$): Even with appropriate treatment, 10–20% of survivors have serious complications or long-term sequelae. Therefore,

$$\wedge = \frac{15}{100} = 0.15.$$

The summary of the estimated model parameter values and the relative sources is given in Table 3.

Table 3. Model parameter values.

Parameter	Value	Source
α	211	Estimated
μ	0.000043	Estimated
ω_1	0.000547	Estimated
ω_2	0.00068	Estimated
β	0.88	[21]
γ_{C1}	0.143	Estimated
γ_{C2}	0.3	[13]
γ_{I1}	0.125	Estimated
γ_{I2}	0.1	[13]
η	0.75	Assumed
δ	0.43	Estimated
ϵ_1	0.85	[1]
ϵ_2	0.90	[1]
σ_1	0.5	Estimated
σ_2	0.25	Estimated
τ_1	0.3	[23]
τ_2	0.5	Assumed
θ_1	0.2	Assumed
θ_2	0.5	[13]
ρ_1	0.85	[23]
ρ_2	0.9	Assumed
$\wedge$	0.15	Estimated

3.5. Estimated $\mathcal{R}_0$ value and herd immunity

Using the model parameter values given in Table 3, the estimated value of $\mathcal{R}_{01}$ is approximately 1.3409, while that of $\mathcal{R}_{02}$ is 0.4853. Therefore,

$$\mathcal{R}_0 = \max\{\mathcal{R}_{01}, \mathcal{R}_{02}\} = \max\{1.3409, 0.4853\} = 1.3409.$$

From a biological perspective, this threshold value indicates that bacterial meningitis has high potential to invade a population if no control efforts are implemented to curtail the transmission and spread of the disease. Therefore, it is important to determine the proportion of the population that needs to be immunized to prevent large outbreaks of bacterial meningitis in Ghana. When a large-scale population is immunized against a contagious infectious disease (either by vaccination or recovery from the infection), indirect protection is provided to the remaining population, which is not immune to the disease. This type of protection is referred to as herd immunity [33, 34]. Herd immunity plays a major role in epidemic control by providing a better understanding of the effectiveness of vaccination without reaching 100% population coverage.

Therefore, the critical level of population immunity, denoted by $\hat{p}$, is calculated with respect to the estimated $\mathcal{R}_0$

value for Ghana's bacterial meningitis outbreaks as

$$\hat{p} = 1 - \frac{1}{\mathcal{R}_0} = 0.25. \tag{3.44}$$

This finding implies that bacterial meningitis will not spread if at least 25% of the population is immune to the disease. Hence, successful vaccination of approximately 25% of the entire population of both strains may lead to eradication of the disease in Ghana.

3.6. Sensitivity analysis

In the mathematical modeling of infectious diseases, it is pertinent to determine the major model parameters that affect disease transmission. Sensitivity analysis aids in identifying parameters that have a high impact on the basic reproduction number, thereby providing insight into the parameters to be considered for control strategies. Following [29], the standardized forward sensitivity index was employed to carry out a sensitivity analysis of model (2.13). The standardized forward sensitivity index of $\mathcal{R}_0$ with respect to parameter ψ is the proportion of the relative change in ψ. Therefore, Table 4 provides all the model parameters that are partially differentiable with respect to $\mathcal{R}_{01}$ and $\mathcal{R}_{02}$, their values, and the sensitivity indices with respect to each strain.

Table 4. Sensitivity indices (SI) of each model parameter on $\mathcal{R}_{01}$ and $\mathcal{R}_{02}$.

Parameter	Value	SI for strain 1	SI for strain 2
μ	0.000043	$+1.93 \times 10^{-3}$	-6.28×10^{-3}
ω_1	0.000547	+0.1362	−0.4413
ω_2	0.00068	−0.1376	+0.4507
β	0.88	+1	+1
γ_{C1}	0.143	-1.14×10^{-2}	⋯
γ_{C2}	0.3	⋯	−0.1775
γ_{I1}	0.125	−0.2200	⋯
γ_{I2}	0.1	⋯	−0.1510
η	0.75	+0.0232	+0.1998
δ	0.43	−0.7567	−0.6492
ϵ_1	0.85	−0.2816	⋯
ϵ_2	0.90	⋯	−2.9077
σ_1	0.5	-1.18×10^{-2}	⋯
σ_2	0.25	⋯	-2.23×10^{-2}
τ_1	0.3	-1.75×10^{-4}	⋯
τ_2	0.5	⋯	-3.52×10^{-4}
θ_1	0.1	−0.1469	+0.4760
θ_2	0.5	+0.1463	−0.4791

3.6.1. Description of the sensitivity indices on $\mathcal{R}_{01}$ and $\mathcal{R}_{02}$

The sensitivity indices for strain 1 show that when the parameters μ, ω_1, β, η and θ_2 are increased, keeping all other parameters constant, the value of $\mathcal{R}_{01}$ is increased, thereby increasing the endemicity of the disease, as they have positive indices. In contrast, the parameters ω_2, γ_{C1}, γ_{I1}, δ, ϵ_1, σ_1, τ_1 and θ_1 decrease the value of $\mathcal{R}_{01}$ when increased, with all other parameters held constant, resulting in a decrease in the endemicity of the disease as they have negative indices. Similarly, for strain 2, when parameters ω_2, β, η and θ_1 are increased, keeping all other parameters constant, the value of $\mathcal{R}_{02}$ is increased, resulting in an increase in the endemicity of the disease, as they have positive indices. The parameters μ, ω_1, γ_{C2}, γ_{I2}, δ, ϵ_2, σ_2, τ_2 and θ_2, on the other hand, decrease the value of $\mathcal{R}_{02}$ when increased, with all other parameters held constant, thereby decreasing the endemicity of the disease as they have negative indices. For instance, increasing the vaccine waning rate of strain 1, ω_1, by 10% will lead to a 1.362% increase in $\mathcal{R}_{01}$, whereas increasing the recovery rate of the carriers of strain 2, γ_{C2}, by 10% will result in a reduction of 1.775% on $\mathcal{R}_{02}$.

4. Numerical simulation of the model

The numerical solution of model (2.13) is obtained using the MATLAB ODE 45 algorithm for solving non-stiff system of ordinary differential equations with initial conditions and parameter values, as shown in Table 3. The graphs of each model compartment against time are presented, with time ranging from 0 to 30 days.

Figure 3 indicates that the susceptible population starts to decrease after 11 days due to the forces of infection for strains 1 and 2. It can be observed from this compartment that an increase in the vaccine uptake rates for both strains, θ_1, θ_2, leads to a rapid decrease in the population. Hence, the awareness of the affected population to be vaccinated decreases susceptibility. Figure 4 shows the vaccinated population of strains 1 and 2 at vaccine uptake rates of $\theta_1, \theta_2 = 0$. This presents a steady-state solution for both compartments. In Figure 5, the population increased at a faster rate within 15 days owing to inflow from the susceptible compartment. Thereafter, an equilibrium point

was reached, and the population began to decrease due to the progression of the carriers to the infected population, as the average incubation period of strain 1 infection is 2 days. This decrease can also be due to the recovery of carriers from the infection, because an increase in the recovery rate of carriers of strain 1, γ_{C1}, leads to a decrease in the population.

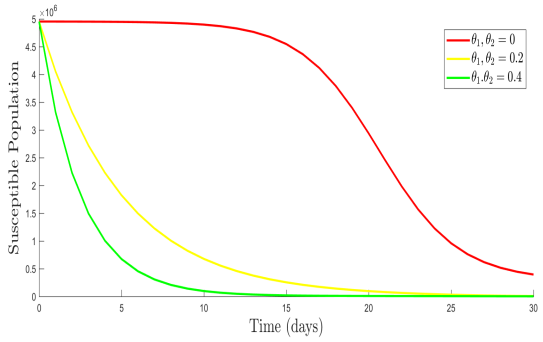

Figure 3. Evolution of susceptible population varying θ_1, θ_2.

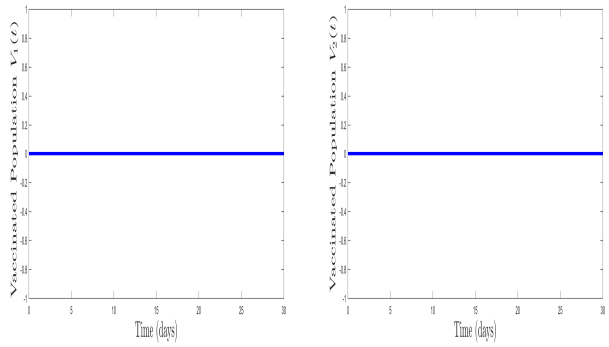

(a) Evolution of $V_1(t)$. **(b)** Evolution of $V_2(t)$.

Figure 4. Vaccinated populations of strain 1 and 2 against time.

Figure 6 also shows an increase in population as a result of susceptible becoming a carrier. The population achieves stationarity momentarily and begins to decrease as the carriers progress to the infected population, since the average incubation period of strain 2 infection is 4 days. The population also decreased owing to the recovery of the carriers. It can be seen that an increase in the recovery rate of carriers of strain 2, γ_{C2}, drastically reduces the population.

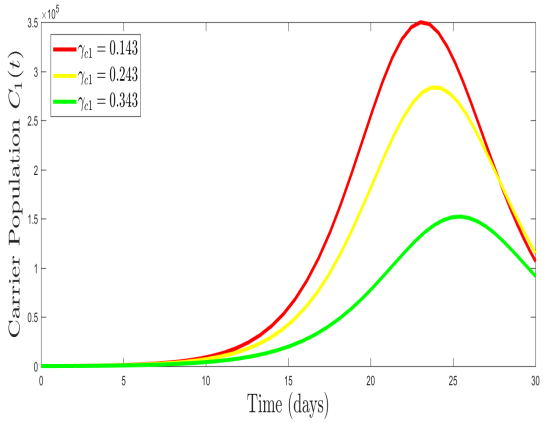

Figure 5. Evolution of carrier population of strain 1.

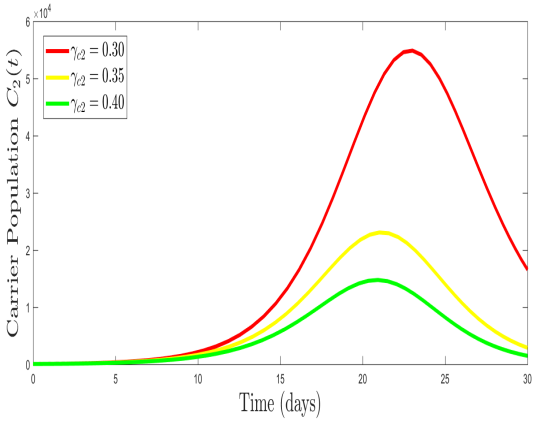

Figure 6. Evolution of carrier population of strain 2.

Figure 7 shows an increase in the infected population of strain 1 as a result of the movement of its susceptible and carrier population. However, population size decreased after this period. This decrease can be ascribed to the availability of treatment for infected compartments since they are symptomatic and can be easily diagnosed. It also decreases due to recovery from infection and disease-induced death. It can be observed that an increase in the recovery rate of infected population of strain 1, γ_{I1} decreases the population. The infected population of strain 2 in Figure 8 increased because of inflow from the susceptible and carrier populations. The population achieves stationarity momentarily and begins to decrease owing to recovery from

infection and disease-induced death. This decrease can also be attributed to the population receiving urgent treatment since the disease is considered a medical emergency. In addition, an increase in the recovery rate of infected with strain 2, γ_{I2}, rapidly decreases the population.

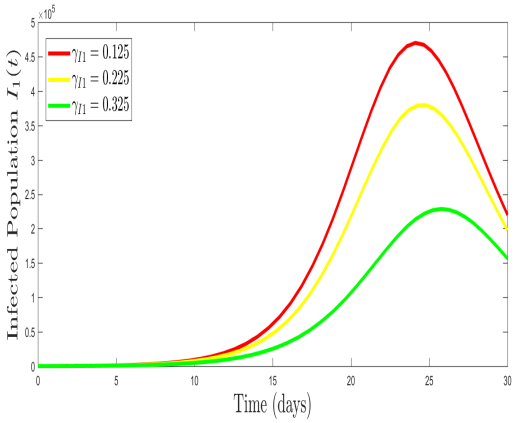

Figure 7. Evolution of infected population of strain 1.

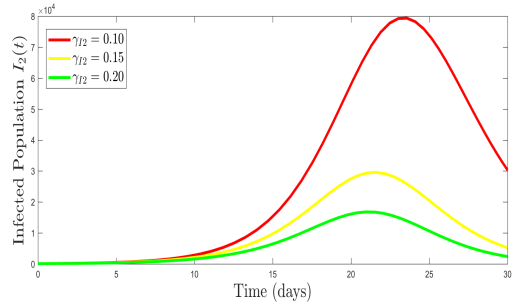

Figure 8. Evolution of infected population of strain 2.

In Figure 9, the fully recovered population maintained a stable state for the first 10 days, then began to increase afterwards. This is because at the onset of the disease, there were no recovered individuals, so as they became infected and recovered, the population increased. Thereafter, we observed a small decrease in the population, which can be attributed to those who recovered from the acute phase of the disease and only found that they experienced some difficulties/complications. The recovered population with complications in Figure 10 also showed a stable state for the first 12 days and a sharp increase over time. It can be observed that an increase in the recovery rates of strains 1 and 2, γ_{I1}, γ_{I2}, leads to a decrease in the population.

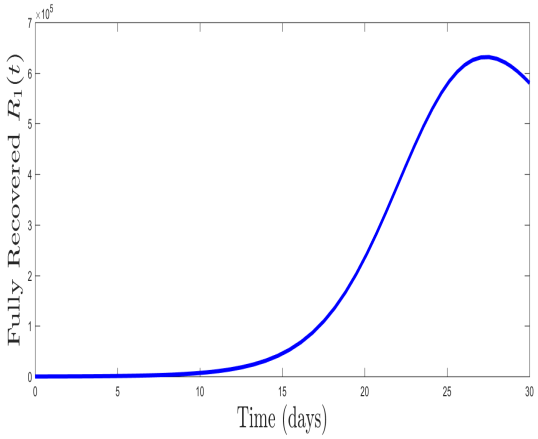

Figure 9. Evolution of fully recovered population from both strains.

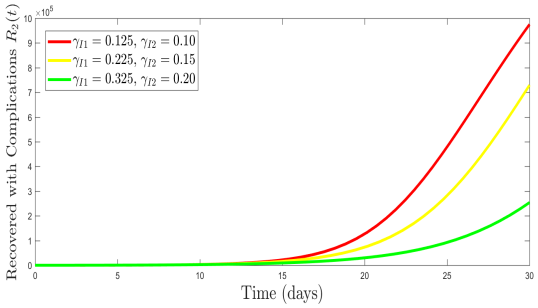

Figure 10. Evolution of recovered with complications from both strains.

4.1. Effects of varying the vaccine uptake rates θ_1 and θ_2

Varying θ_1 to the vaccinated population with immunity to strain 1 resulted in a sharp increase in the population within the first 3 days, as shown in Figure 11(a). This result is in agreement with those of [22, 23]. Moreover, a stable state was achieved in the following days as the population became immune to the specific strain. However, by varying θ_1, the carrier population of strain 1 decreases, indicating that increasing the number of vaccinated individuals reduced the number of carriers. Varying θ_1 on the infected population of strain 1 shows a rapid decrease in the population, which reveals that the more people receive the vaccine, the lower is the infection. The variation in θ_1 in the recovered population

with complications also showed a dramatic decrease in the population. This can be attributed to the immune response of the human body to recognize and fight bacteria after vaccination. The variation in θ_2 in the vaccinated

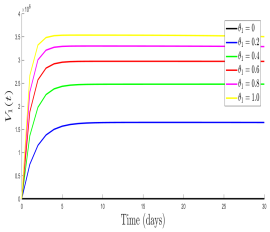

(a) Effects of varying θ_1 on $V_1(t)$.

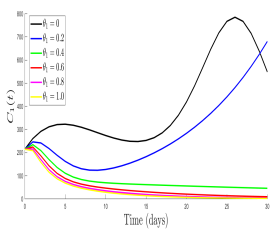

(b) Effects of varying θ_1 on $C_1(t)$.

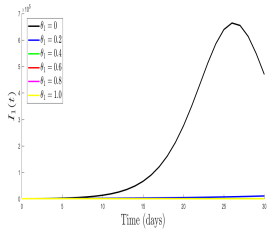

(c) Effects of varying θ_1 on $I_1(t)$.

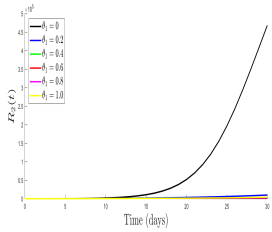

(d) Effects of varying θ_1 on $R_2(t)$.

Figure 11. Effects of varying θ_1 on $V_1(t)$, $C_1(t)$, $I_1(t)$ and $R_2(t)$ compartments.

population with immunity to strain 2 displays a surge in the population within the first 3 days and achieves stability as the population becomes immune to the specified strain, as shown in Figure 12(a). Varying θ_2 on the carrier population of strain 2 decreases the population as the vaccine uptake rate increased. As θ_2 varies with the infected population of strain 2, a sharp decrease is observed, indicating the impact of vaccination on curtailing infection. Varying θ_2 on the recovered population with complications shows a rapid decrease in the population, which means that the more we get vaccinated, the fewer are the complications after an acute infection.

5. Conclusions

This study proposes a novel deterministic model of a coupled system of nine ordinary differential equations for the transmission dynamics of two-strain bacterial

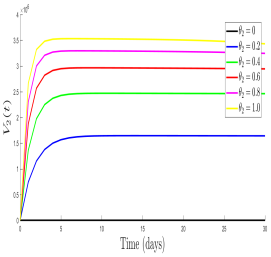

(a) Effects of varying θ_2 on $V_2(t)$.

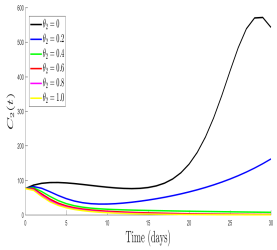

(b) Effects of varying θ_2 on $C_2(t)$.

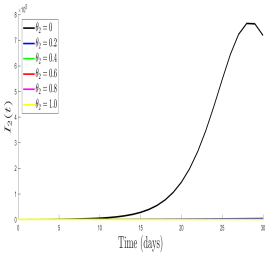

(c) Effects of varying θ_2 on $I_2(t)$.

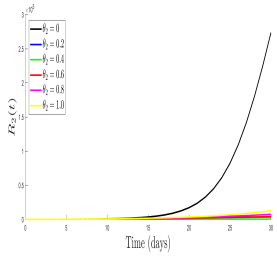

(d) Effects of varying θ_2 on $R_2(t)$.

Figure 12. Effects of varying θ_2 on $V_2(t)$, $C_2(t)$, $I_2(t)$ and $R_2(t)$ compartments.

meningitis. The introduction of vaccination populations against strains 1 and 2 accounts for most of the total population, thereby curbing the spread of infections. Positivity analysis of the two-strain model showed that it is epidemiologically feasible and represents what can be obtainable in real life. The mathematical analysis of the model shows that the model has a DFE that is locally and globally asymptotically stable if $\mathcal{R}_{01}, \mathcal{R}_{02} < 1$, and unstable if $\mathcal{R}_{01}, \mathcal{R}_{02} > 1$. The basic reproduction number indicates that with herd immunity of 25%, the disease can be eradicated over a certain period of time, as represented in the numerical simulation results. The robustness of the model predictions to the parameter values was examined via a sensitivity analysis, which established that the transmission probability, β is an effective contributor to $\mathcal{R}_0$, which is essential for the spread and control of the disease.

Use of AI tools declaration

The authors declare they have not used Artificial Intelligence (AI) tools in the creation of this article.

Conflicts of interest

The authors declare that they have no conflicts of interest in this paper.

References

1. World Health Organization, Meningitis, World Health Organization, 2020. Available from: http://www.who.int/health-topics/meningitis.
2. A. R. Tunkel, B. J. Hartman, S. L. Kaplan, B. A. Kaufman, K. L. Roos, W. M. Scheld, et al., Practice guidelines for the management of bacterial meningitis, *Clin. Infect. Dis.*, **39** (2004), 1267–1284. https://doi.org/10.1086/425368
3. L. Ginsberg, Difficult and recurrent meningitis, *J. Neurol. Neurosurg. Psychiatry*, **75** (2004), i16–i21. http://doi.org/10.1136/jnnp.2003.034272
4. C. W. Woods, G. Armstrong, S. O. Sackey, C. Tetteh, S. Bugri, B. A. Perkins, et al., Emergency vaccination against epidemic meningitis in Ghana: implications for the control of meningococcal disease in West Africa, *Lancet*, **335** (2000), 30–33. https://doi.org/10.1016/S0140-6736(99)03366-8
5. T. Letsa, C. L. Noora, G. K. Kuma, E. Asiedu, G. Kye-Duodu, E. Afari, et al., Pneumococcal meningitis outbreak and associated factors in six districts of Brong Ahafo Region, Ghana, 2016, *BMC Public Health*, **18** (2018), 781. https://doi.org/10.1186/s12889-018-5529-z
6. N. Amidu, B. B. Antuamwine, O. Addai-Mensah, A. Abdul-Karim, A. Stebleson, B. B. Abubakari, et al., Diagnosis of bacterial meningitis in Ghana: polymerase chain reaction versus latex agglutination methods, *PLoS One*, **14** (2019), e0210812. https://doi.org/10.1371/journal.pone.0210812
7. Centre for Disease Control, Meningitis in West Africa, Centre for Disease Control, 2021. Available from: http://wwwnc.cdc.gov/travel/yellowbook/2010/chapter-2/meningococcal-disease.aspx.
8. L. Fordjour, R. Abdul-Razak, Ghana: UWR records 18 deaths from meningitis within 10 weeks, *Ghanaian Times*, 2020. Available from: https://allafrica.com/stories/202003170696.html.
9. B. Dartey, O. Afreh, E. Teviu, G. Khumalo, T. Letsa, K. Issah, et al., Analysis of meningitis outbreak data, Jaman North district, Brong Ahafo Region, *Ghana Med. J.*, **54** (2020), 53–58. https://doi.org/10.4314/gmj.v54i2s.9
10. B. B. Kaburi, C. Kubio, E. Kenu, D. K. Ameme, J. K. Mahama, S. O. Sackey, et al., Evaluation of bacterial meningitis surveillance data of the northern region, Ghana, 2010–2015, *Pan Afr. Med. J.*, **27** (2017), 11036. https://doi.org/10.11604/pamj.2017.27.164.11036
11. T. J. Irving, K. B. Blyuss, C. Colijn, C. L. Trotter, Modelling meningococcal meningitis in the African meningitis belt, *Epidemiol. Infect.*, **140** (2012), 897–905. https://doi.org/10.1017/S0950268811001385
12. M. Martcheva, G. Crispino-O'Connell, The transmission of meningococcal infection: a mathematical study, *J. Math. Anal. Appl.*, **283** (2003), 251–275. https://doi.org/10.1016/S0022-247X(03)00289-0
13. E. N. Wiah, I. A. Adetunde, A mathematical model of cerebrospinal meningitis epidemic: a case study for Jirapa district, Ghana, *Curr. Appl. Sci. Technol.*, **10** (2010), 63–73.
14. T. T. Yusuf, A. O. Olayinka, Optimal control of meningococcal meningitis transmission dynamics: a case study of Nigeria, *IOSR J. Math.*, **15** (2019), 13–26.
15. World Health Organization, Meningococcal meningitis, World Health Organization, 2018. Available from: https://www.who.int/news-room/fact-sheets/detail/meningococcal-meningitis.
16. S. Tartof, A. Cohn, F. Tarbangdo, M. H. Djingarey, N. Messonnier, T. A. Clark, et al., Identifying optimal vaccination strategies for serogroup A Neisseria meningitidis conjugate vaccine in the African meningitis belt, *PLoS One*, **8** (2013), e63605. https://doi.org/10.1371/journal.pone.0063605
17. S. Tartof, A. Cohn, F. Tarbangdo, M. H. Djingarey, N. Messonnier, T. A. Clark, et al., Correction: identifying optimal vaccination strategies for serogroup a Neisseria meningitidis conjugate vaccine in the African meningitis belt, *PLoS One*, **12** (2017), e0190188. https://doi.org/10.1371/journal.pone.0190188

18. K. B. Blyuss, Mathematical modelling of the dynamics of meningococcal meningitis in Africa, In: P. J. Aston, A. J. Mulholland, K. M. M. Tant, *UK success stories in industrial mathematics*, 2016, 221–226. https://doi.org/10.1007/978-3-319-25454-8_28
19. T. T. Yusuf, Mathematical modelling and simulation of meningococcal meningitis transmission dynamics, *FUTA J. Res. Sci.*, **14** (2018), 94–104.
20. M. J. F. Martinez, E. G. Merino, E. G. Sanchez, J. E. G. Sanchez, M. del Rey, G. R. Sanchez, A mathematical model to study the meningococcal meningitis, *Proc. Comput. Sci.*, **18** (2013), 2492–2495. https://doi.org/10.1016/j.procs.2013.05.426
21. J. J. K. Asamoah, F. Nyabadza, B. Seidu, M. Chand, H. Dutta, Mathematical modelling of bacterial meningitis transmission dynamics with control measures, *Comput. Math. Methods Med.*, **2018** (2018), 2657461. https://doi.org/10.1155/2018/2657461
22. F. B. Agusto, M. C. A. Leite, Optimal control and cost-effective analysis of the 2017 meningitis outbreak in Nigeria, *Infect. Dis. Modell.*, **4** (2019), 161–187. https://doi.org/10.1016/j.idm.2019.05.003
23. I. M. ELmojtaba, S. O. Adam, A mathematical model for meningitis disease, *Red Sea Univ. J. Basic Appl. Sci.*, **2** (2017), 467–472.
24. M. V. Crankson, O. Olotu, N. Amegbey, A. S. Afolabi, Mathematical modeling and stability analyses on the transmission dynamics of bacterial meningitis, *J. Math. Comput. Sci.*, **11** (2021), 7384–7413. https://doi.org/10.28919/jmcs/6513
25. P. Apanga, J. Awoonor-Williams, An evaluation of the meningitis surveillance in northern Ghana, *Int. J. Trop. Dis. Health*, **12** (2016), 1–10. https://doi.org/10.9734/IJTDH/2016/22489
26. World Health Organization, Meningococcal Meningitis, World Health Organization, 2020. Available from: https://www.who.int/news-room/fact-sheets/detail/meningococcal-meningitis.
27. M. Barik, S. Chauhan, S. K. Bhatia, Efficacy of pulse vaccination over constant vaccination in COVID-19: a dynamical analysis, *Commun. Math. Biol. Neurosci.*, **94** (2020), 1–33. https://doi.org/10.28919/cmbn/5187
28. S. Chauhan, O. P. Misra, J. Dhar, Stability analysis of SIR model with vaccination, *Amer. J. Comput. Appl. Math.*, **4** (2014), 17–23. https://doi.org/10.5923/j.ajcam.20140401.03
29. A. Abidemi, M. I. Abd-Aziz, R. Ahmad, Vaccination and vector control effect on dengue virus transmission dynamics: modelling and simulation, *Chaos Solitons Fract.*, **133** (2020), 109648. https://doi.org/10.1016/j.chaos.2020.109648
30. C. Castillo-Chavez, Z. Feng, W. Huang, On the computation of R_0 and its role on global stability, In: *Mathematical approaches for emerging and re-emerging infectious diseases: an introduction*, 2002, 229–250. https://doi.org/10.1007/978-1-4757-3667-0_13
31. Ghana Statistical Service, Population Size Ghana, by Region, 2010–2020, Ghana Statistical Service, 2020. Available from: https://statsghana.gov.gh/.
32. A. Z. Trestioreanu, A. Fraser, A. Gafter-Gvili, M. Paul, L. Leibovici, Antibiotics for preventing meningococcal infections, *Cochrane Database Syst. Rev.*, **10** (2013), 1–47. https://doi.org/10.1002/14651858.CD004785.pub5
33. K. O. Kwok, F. Lai, W. I. Wei, S. Y. S. Wong, J. W. Tang, Herd immunity-estimating the level required to halt the COVID-19 epidemics in affected countries, *J. Infect.*, **80** (2020), e32–e33. https://doi.org/10.1016/j.jinf.2020.03.027
34. A. Abidemi, Z. M. Zainuddin, N. A. B. Aziz, Impact of control interventions on COVID-19 population dynamics in Malaysia: a mathematical study, *Eur. Phys. J. Plus*, **136** (2021), 237. https://doi.org/10.1140/epjp/s13360-021-01205-5

AIMS Press